Chapter 10

Output Power of Laser Resonators

10.1 Output Power of Stable Resonators

10.1.1 Linear Resonators

The differential equations (9.35) and (9.56) describing the amplification of the intensity inside the active medium are now used to derive the output power of stable resonators. In the resonator model used (Fig. 10.1) it is assumed that both the forward travelling beam with intensity $I^+(z)$ and the backward traveling beam with intensity $I^-(z)$ cover the same area of the active medium. The complete overlap of the two counterpropagating beams is characteristic for stable resonators. During a round trip the intensity is decreased due to diffraction losses (loss factors V_1-V_4), scattering, and absorption inside the medium (loss factor V_S), and by output coupling. In steady state operation, these losses are compensated by the amplification process characterized by the small-signal gain coefficient g_0. The next assumption we make is that no spatial hole burning is present meaning that at any plane inside the medium the intensity $I(z)$ is given by the sum of the two intensities $I^+(z)$ and $I^-(z)$. This is a reasonable approach for most lasers since the effect of spatial hole burning on the output power is smoothed out by atomic motion (gas lasers), energy migration, or axial multimode operation (solid state lasers). Furthermore, the mode is assumed to exhibit a flat-top intensity profile. The incorporation of the real mode structure will be discussed in Chapter 11.

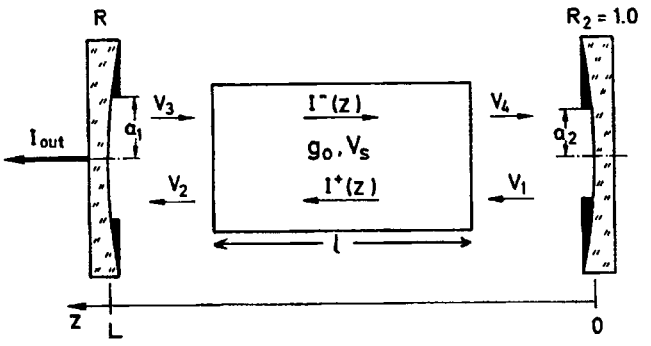

Fig. 10.1 Resonator model used for the calculation of the output power. The intensity is decreased by the diffraction loss factors V_1-V_4 (=1-loss), the loss factor per transit V_S of the medium, and the reflectance R of the output coupling mirror.

However, in single axial mode solid state or liquid dye lasers, spatial hole burning has an impact on the output power (it is lower by up to 30%). In these cases a realistic model for the output power requires the incorporation of the interference between the two counterpropagating fields resulting in the intensity profile:

$$I(z) = I^{+}(z) + I^{-}(z) - 2\sqrt{I^{+}(z)I^{-}(z)}\cos[2kz] \tag{10.1}$$

with k being the wave number inside the medium. Without spatial hole burning, the differential equations for the intensities according to (9.35) and (9.56) read [4.1,4.3,4.11]:

$$\frac{dI^{\pm}(z)}{dz} = \pm\left[\frac{g_0}{\left(1 + \dfrac{I^{+}(z) + I^{-}(z)}{I_S}\right)^{X}} - \alpha_0\right] I^{\pm}(z) \tag{10.2}$$

where g_0 is the small-signal gain coefficient, I_S is the saturation intensity, α_0 is the loss coefficient, and X is equal to 1.0 (0.5) for homogeneous (inhomogeneous) broadening.

Before we solve these equations to obtain the intensity $I^{+}(L)$, which is proportional to the output power P_{out}, let us derive an approximate solution by assuming that the intensity sum in (10.2) is constant with $I^{+}(z)+I^{-}(z)=2I$. The mean intensity I now represents the intensity of the beam traveling towards the output coupling mirror. Equation (10.2) then yields for the factor GV_S by which the intensity is amplified in a transit through the medium:

$$GV_S = \exp\left[\frac{g_0\ell}{(1 + 2I/I_S)^{X}}\right]\exp\left[-\alpha_0\ell\right] \tag{10.3}$$

By using the steady state condition:

$$G^2RV_S^2V_1V_2V_3V_4 = 1 \tag{10.4}$$

the intensity I is found to be:

$$I = \frac{I_S}{2}\left[\left(\frac{g_0\ell}{\left|\ln\sqrt{RV_S^2V_1V_2V_3V_4}\right|}\right)^{\frac{1}{X}} - 1\right] \tag{10.5}$$

If the cross sectional area of the beam is A_b ($=\pi a_1^2$ in Fig. 10.1), the output power is given by:

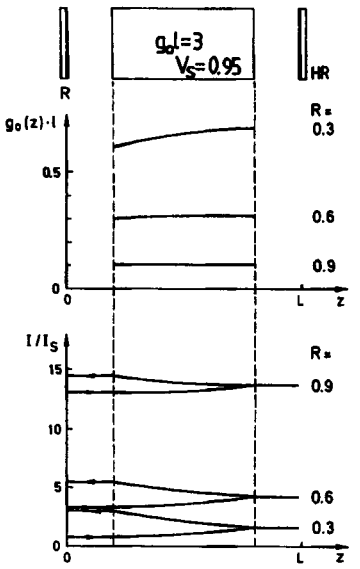

Fig. 10.2 Gain *lnG* and intensities as a function of the axial coordinate *z* for different reflectances *R* of the output coupler, calculated with (10.2) ($g_0\ell$=1.5, $\alpha_0\ell$=0.053, no diffraction losses).

$$P_{out} = A_b\, I\, (1-R)V_2 = A_b\, I_S \frac{(1-R)V_2}{2\left(\left|\ln\sqrt{RV_S^2V}\right|\right)^{\frac{1}{x}}} \left[(g_0\ell)^{\frac{1}{x}} - \left(\left|\ln\sqrt{RV_S^2V}\right|\right)^{\frac{1}{x}}\right] \qquad (10.6)$$

with the round trip diffraction loss factor $V=V_1V_2V_3V_4$. This expression for the output power of stable resonators can be used to a very good approximation, if the output coupling is low (high reflectance, $R>0.7$). In this case the sum of the two intensities inside the medium is almost constant as a numerically calculated example in Fig. 10.2 indicates. For lower reflectances, the z-dependence of the intensities has to be taken into account by solving the differential equation (10.2) using the boundary conditions at the mirrors. Unfortunately, the solution can only be found numerically due to the homogeneously distributed loss (loss coefficient α_0) inside the medium [4.11-4.13]. However, for homogeneously broadened lasers ($x=1$) it is possible to derive an analytical solution by setting α_0 equal to zero in (10.2) and taking into account the loss by multiplying the intensity at the high reflecting mirror with the loss factor $V_S^2=exp[-2\alpha_0\ell]$. This method provides an analytical expression for the output power that is very close to the numerical solution (the difference is less than 0.5%). After a lengthy calculation the final expression reads [4.18]:

$$P_{out} = A_b\, I_S \frac{(1-R)V_2}{1 - RV_2V_3 + \sqrt{RV}\,(1/(V_1V_2V_3) - V_3)} \left|g_0\ell - \left|\ln\sqrt{RV_S^2V}\right|\right| \qquad (10.7)$$

with: $V = V_1 V_2 V_3 V_4$.

A comparison with (10.6) indicates that the z-dependence of the gain leads to a change in the fraction. For high reflectances R both equations provide similar output powers. In the following we use a simplified version of (10.7) by ignoring the diffraction losses. We thus consider a resonator that exhibits a loss factor per transit V_S. Equation (10.7) then reads:

$$P_{out} = A_b\, I_S \frac{1-R}{1 - R + \sqrt{R}\,(1/V_S - V_S)} \left[g_0 \ell - \left|\ln\sqrt{R V_S^2}\right|\right] \tag{10.8}$$

Figure 10.3 presents the normalized output power $P_{out}/(A_b I_S)$ as a function of the small-signal gain $g_0\ell$ which for most laser materials is proportional to the pump power. Starting at the threshold small-signal gain $(g_0\ell)_{th} = |\ln(\sqrt{R}V_S)|$ the power increases linearly with the small-signal gain and the slope of the curve becomes steeper as the reflectance R of the output coupler is decreased. The output power cannot exceed the power P_{OL} that is available in the medium in the form of inversion, with (Sec. 9.3):

$$P_{OL} = A\, I_S\, g_0\ell = \eta_{excit}\, P_{pump} \tag{10.9}$$

with:

A	:	cross sectional area of the medium
η_{excit}	:	excitation efficiency
P_{pump}	:	pump power

Only if the laser resonator exhibits no losses (V_S=*1.0* and R-->*1.0* in (10.8)) and the laser beam fills the whole medium (A_b=A) can all the available power P_{OL} be extracted from the active medium (broken line in Fig. 10.3). Note that (10.9) holds only for homogeneously broadened lasers. For inhomogeneous line broadening, the available power is a function of the laser intensity due to the broadening of the homogeneous line width (see Sec. 9.5).

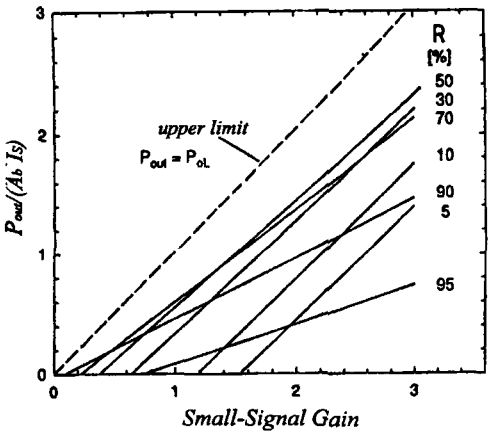

Fig. 10.3 Normalized laser power as a function of the small-signal gain for different reflectances of the output coupler according to (10.8) assuming a loss per transit of 5% (V_S=0.95).

The slope of the output power with respect to the electrical pump power is referred to as the slope efficiency η_{slope} with:

$$\eta_{slope} = \frac{dP_{out}}{dP_{pump}} = \eta_{excit} \frac{dP_{out}}{A\, I_S\, d(g_0 \ell)}$$

$$= \eta_{excit}\, \gamma \frac{1 - R}{1 - R + \sqrt{R}(1/V_S - V_S)} \tag{10.10}$$

where $\gamma = A_i/A$ is the fill factor. The slope efficiency is a function of the loss, the output coupling, and the ratio of the mode volume to the volume of the active medium. This ratio, called the fill factor, can be calculated in a first approach by using the beam diameter of the highest order mode inside the active medium. If the active medium represents the only aperture inside the stable resonator and a high enough number of transverse modes are able to oscillate (let us say more than 10), the maximum fill factor of 1.0 is obtained. In fundamental mode operation with the Gaussian beam radius w being adapted to the radius b of the active medium ($b \approx 1.3w$), the fill factor typically is around 0.9.

Unless the resonator exhibits no losses, only a fraction of the maximally available power P_{OL} can be extracted in the form of a laser beam. This fraction is referred to as the extraction efficiency η_{extr} of the resonator:

$$\eta_{extr} = \frac{P_{out}}{P_{OL}} = \frac{1}{\eta_{excit}} \frac{P_{out}}{P_{pump}} \tag{10.11}$$

The total efficiency of the laser resonator is given by:

$$\eta_{tot} = \frac{P_{out}}{P_{electr}} = \eta_{excit}\, \eta_{extr} \tag{10.12}$$

Example: cw Nd:YAG laser ($I_S = 2kW/cm^2$), rod diameter: 10mm ($A = 0.785cm^2$), multimode operation ($\gamma = 1.0$), electrical pump power : 10 kW. The loss factor per transit and the small-signal gain were determined experimentally (see Chapter 23) to be $V_S = 0.95$ and $g_0\ell = 0.04$ per kW of pump power. According to (10.9), this corresponds to an excitation efficiency of 6.28%. Using (10.8) the following output powers, extraction efficiencies, and total efficiencies are to be expected:

R	0.6	0.7	0.8	0.9	0.95
P_{out} [W]	122	208	255	235	169
η_{extr} [%]	19.5	33.1	40.6	37.5	26.9
η_{tot} [%]	1.22	2.08	2.55	2.35	1.69

Optimum Output Coupling and Maximum Output Power

If the reflectance of the output coupler is varied at a given small-signal gain or pump power, the output power exhibits a maximum at the optimum output coupling. This behavior is easy to understand considering the fact that the output power is zero at low reflectances (laser threshold is not reached) and at a reflectance of 100% (no power is coupled out of the resonator). Thus a maximum of the output power and the extraction efficiency must exist for a certain value of the output coupling. Going back to our approximate power formula (10.6) we can find the optimum reflectance R_{opt} and the maximum output power $P_{out,max}$ by setting the derivative $\delta P_{out}/\delta(lnR)$ equal to zero. Again, we assume that the losses per transit are represented by the loss factor $V_S = exp[-\alpha_0 \ell]$, and we consequently set the diffraction loss factor V equal to 1.0. By using the approximation $1-R \approx |lnR|$, the following expressions are obtained [4.15]:

a) homogeneous line broadening:

Maximum output power:

$$P_{out,max} = A_b\, I_S\, \alpha_0 \ell \left[\sqrt{\frac{g_0 \ell}{\alpha_0 \ell}} - 1\right]^2 \qquad (10.13)$$

$$= \left[\sqrt{\eta_{excit}\, P_{electr}\, A_b/A} - \sqrt{A_b\, I_S\, \alpha_0 \ell}\right]^2$$

Maximum extraction efficiency:

$$\eta_{extr,max} = \frac{\alpha_0 \ell}{g_0 \ell}\left[\sqrt{\frac{g_0 \ell}{\alpha_0 \ell}} - 1\right]^2 \qquad (10.14)$$

Optimum output coupling:

$$lnR_{opt} = -2\alpha_0 \ell \left[\sqrt{\frac{g_0 \ell}{\alpha_0 \ell}} - 1\right] \qquad (10.15)$$

Although (10.6) is only an approximate expression for the output power, the extreme values given by (10.13)-(10.15) can, to a very good approximation, be used to optimize the power performance of a laser system. This can be easily verified in Fig. 10.4 in which the correct extreme values (found by solving numerically the differential equation (10.2)) are shown [4.13]. Even for lasers with high small-signal gain ($g_0 \ell > 3$) and high loss ($\alpha_0 \ell > 0.1$), which require a low reflectance for optimum performance, the difference between the exact extreme values and the ones given by (10.14) and (10.15) is negligible. Note that the graph presented in Fig. 10.4 assumes a fill factor of $\gamma = A_b/A = 1.0$. The optimum parameters for a given laser are represented by the intersecting point of the two curves with constant small-signal gain and constant loss. Again, we find that an extraction efficiciency of 100% is only attainable if the laser exhibits no loss ($\alpha_0 \ell = 0$) and the output coupling is close to zero. As the loss is increased, the extraction efficiency decreases rapidly and the optimum mirror reflectance is shifted to lower values (Fig. 10.5). Figure 10.5 clearly indicates how sensitively the output power reacts to slight increases of the losses. A loss of 5% per transit in a low-gain laser with $g_0 \ell = 0.4$ results in a reduction of the extraction efficiency by a factor of 2! Half the available power P_{OL} gets lost through spontaneous emission.

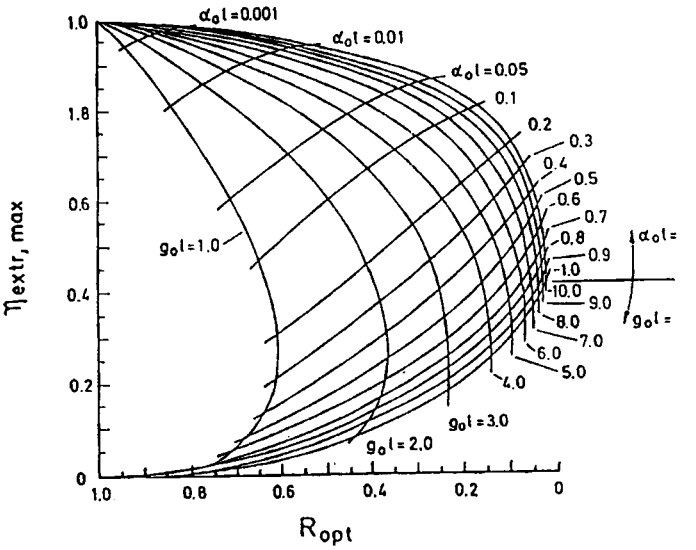

Fig. 10.4 Diagram for the determination of the optimum reflectance R_{opt} and the maximum extraction efficiency $\eta_{extr,max}$ of homogeneously broadened lasers using the small-signal gain $g_0\ell$ and the loss per transit $\alpha_0\ell = -lnV_S$ (fill factor $\gamma = 1.0$) [4.13].

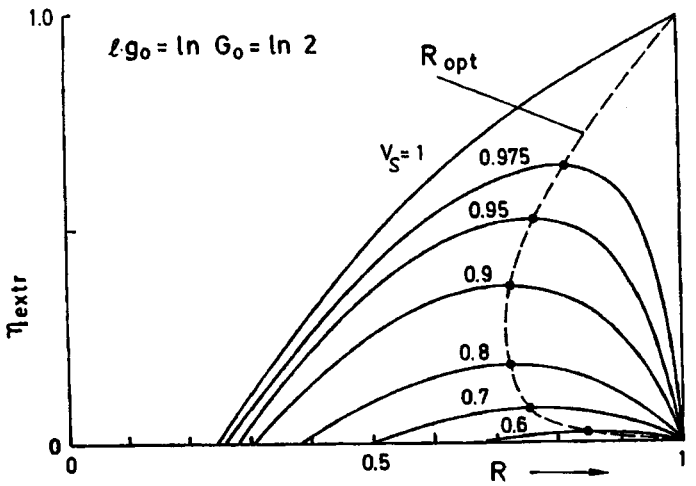

Fig. 10.5 Extraction efficiency as a function of the output coupling reflectance for a small-signal gain of $g_0\ell = ln2$ and different losses per transit. The curve parameter is the loss factor per transit V_S.

The losses have a less dramatic impact on the output power if the small-signal gain of the laser is high. This is why at the same average pump power, lasers provide a higher average output power in pulsed operation than in cw operation. For a repetition rate f and a pulse width Δt, the small-signal gain is higher by the factor $1/(f\Delta t)$ as compared to cw operation at the same average pump power. According to Fig. 10.4, the extraction efficiency is increased leading to a higher average output power. Futhermore, the extraction efficiency becomes less sensitive to changes in output coupling as Fig. 10.6 indicates. The realization of the optimum output coupling is thus much less critical than in a low-gain laser. Figures 10.7 and 10.8 present experimental examples for output power and output energies as a function of the output coupling. In Fig. 10.8 the theoretical curve according to (10.7) is shown too. This example indicates that the expression (10.7) can be used to calculate the output power of a stable resonator if the small-signal gain, the losses, and the fill factor of the resonator are known. The experimental determination of the gain and the loss is easy to accomplish as will be discussed in Chapter 23. The determination of the fill factor, however, is more difficult if only a small number of transverse modes is considered.

In multimode operation the fill factor can, to a good approximation, be calculated by using the cross sectional area of the aperture (see Fig 10.8). If the aperture with radius a is located close to the active medium with radius b, the fill factor is given by:

$$\gamma = \frac{\pi a^2}{\pi b^2} \tag{10.16}$$

For TEM_{00} mode lasers that have the active medium as the limiting aperture, the fill factor is typically around 0.50, meaning that 50% of the multimode power can be extracted in fundamental mode operation. For diode end-pumped TEM_{00} solid state lasers, the fill factor is typically between 0.6 and 0.75, depending on the ratio mode dimaeter to pump spot diameter (typically 0.7-0.9) and aberrations of the thermal lens.

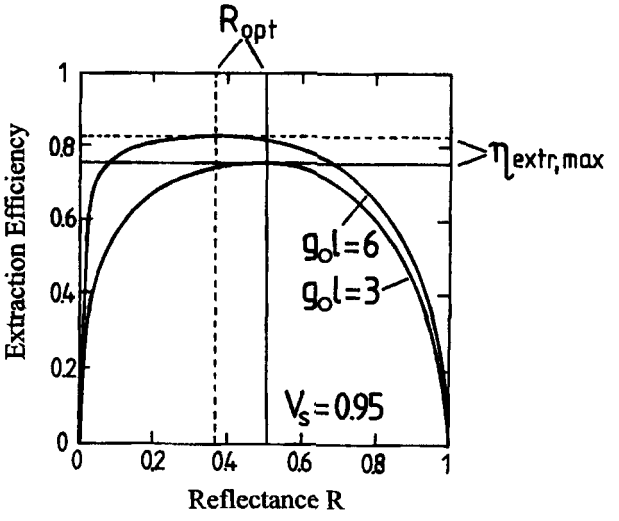

Fig. 10.6 Numerically calculated extraction efficiency as a function of the mirror reflectance R for high small-signal gains. The horizontal and vertical lines mark the analytical values given by (10.14) and (10.15). Loss factor per transit V_S=0.95.

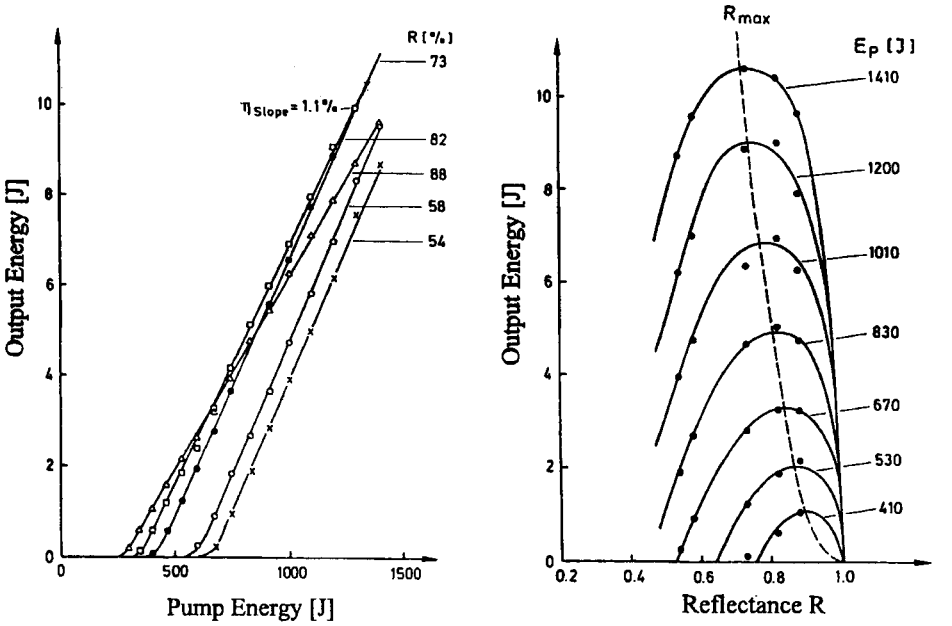

Fig. 10.7 Measured output energy per pulse of Nd:YAG lasers as a function of the pump energy E_p and the output coupling reflectance R [S.11]. The lines represent interpolations.

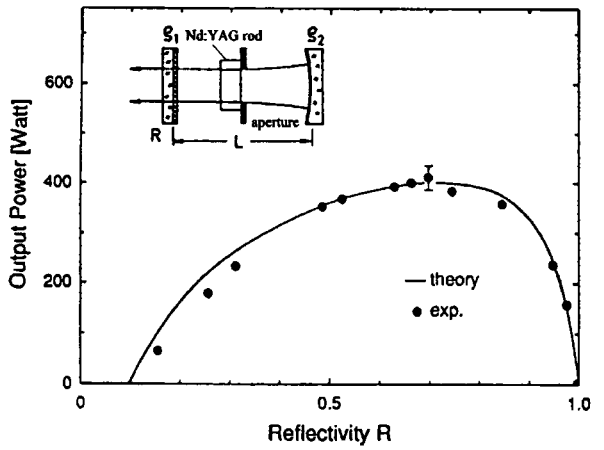

Fig. 10.8 Measured output power of a Nd:YAG laser as a function of the output coupling reflectance. The solid line represents (10.7) with $V_S=0.955$, $V_1=V_4=0.995$, $V_2=V_3=1.0$ ($\rho_1=\infty$, $\rho_2=5m$, $L=1m$, $g_0\ell=1.0$, aperture radius $a=2.8mm$, rod radius $b=3.17mm$).

b) inhomogeneous line broadening:

Maximum output power: $$P_{out,\max} = A_b\, I_S \frac{|\ln R|^2}{\alpha_0 \ell + \ln\sqrt{R}} \tag{10.17}$$

Optimum output coupling: $$[\alpha_0 \ell - \ln\sqrt{R_{opt}}]^3 = (g_0 \ell)^2 [\alpha_0 \ell + \ln\sqrt{R_{opt}}] \tag{10.18}$$

Note that the output power (10.17) is always positive since (10.18) implies that $\alpha_0\ell+\ln\sqrt{R}$ is greater than zero. The output power refers to the power of one single axial mode, and the small-signal gain is generated only by those inverted atoms whose resonance frequencies lie within the homogeneous linewidth around the axial mode frequency. In order to obtain the total output power the contributions of the other axial modes have to be added. Also keep in mind that we based our optimization on (10.6) which is valid for high mirror reflectances only.

10.1.2 Folded Resonators without Beam Overlap

For active media with a large cross section it is sometimes advantageous to fold the resonator by means of high reflecting mirrors or roof prisms as depicted in Fig. 10.9. Folding the resonator N times will decrease the beam diameter by a factor $1/(N+1)$ resulting in an enhancement of the beam quality without decreasing the fill factor. Both the small-signal gain and the loss are now higher by a factor of $N+1$. By using (10.14) and (10.15) for homogeneously broadened lasers and assuming a fill factor of 1.0, we get for the maximum extraction efficiency and the optimum mirror reflectance:

$$\eta_{extr,\max}^{(N)} = \frac{\alpha_0 \ell}{g_0 \ell}\left[\sqrt{\frac{g_0 \ell}{\alpha_0 \ell}} - 1\right]^2 = \eta_{extr,\max}^{(0)} \tag{10.19}$$

$$ln R_{opt}^{(N)} = -2(N+1)\alpha_0 \ell \left[\sqrt{\frac{g_0 \ell}{\alpha_0 \ell}} - 1\right] \tag{10.20}$$

The extraction efficiency does not depend on the number N of folds, and the optimum mirror reflectance is given by the (N+1)th power of the optimum mirror reflectance for the unfolded resonator:

$$R_{opt}^{(N)} = \left[R_{opt}^{(0)}\right]^{N+1} \tag{10.21}$$

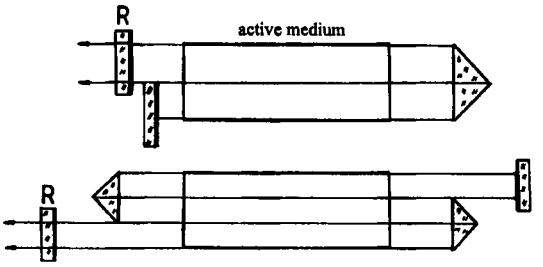

Fig. 10.9 Folded resonators with $N=1$ (top) and $N=2$.

10.1.3 Folded Resonators with Beam Overlap

If the folding is realized such that the different beams are not parallel, they will overlap in certain areas of the active medium. A typical example of such a folding scheme is the tightly folded resonator (TFR) shown in Fig. 10.10 and the slab laser depicted in Fig. 10.11. In order to calculate the output power we first have to determine the influence of the overlapped areas on the extraction efficiency. If the whole beam area is overlapped, the output power will, of course, be decreased by a factor of 2 since the same gain saturation is present for half the laser intensity. As the ratio of the overlapped beam volume to the total beam volume is increased, the normalized extraction efficiency, therefore, will decrease from 100% to 50%. It can be shown numerically that the output power decreases nearly linearly with the ratio of the overlapped mode volume V_{ol} to the total mode volume V_{tot} (Fig. 10.12) [4.19-4.21]. The output power will thus be lower by a factor γ_1 with:

$$\gamma_1 = 1 - 0.5\frac{V_{ol}}{V_{tot}} \tag{10.22}$$

A second correction factor γ_2 takes the increase of the beam cross section from A_b to A_b^*, due to refraction, into account:

$$\gamma_2 = A_b^*/A_b \tag{10.23}$$

Finally, we have to incorporate the longer optical path length ℓ_{zz} (zig-zag) into the expression for the output power. Both the small-signal gain and the loss have to be multiplied by:

$$\gamma_3 = \ell_{zz}/\ell \tag{10.24}$$

with ℓ being the side length of the active medium.

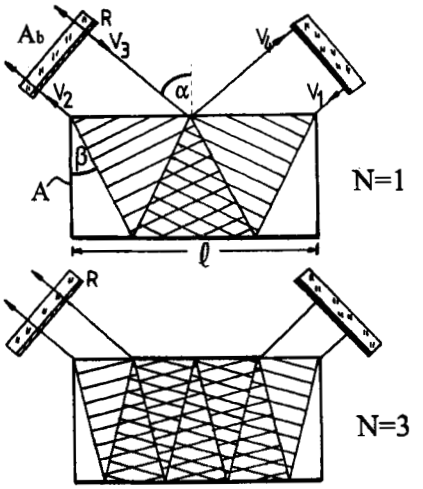

Fig. 10.10 Tightly folded resonators (TFR) with one and three reflections at the bottom surface of the active medium.

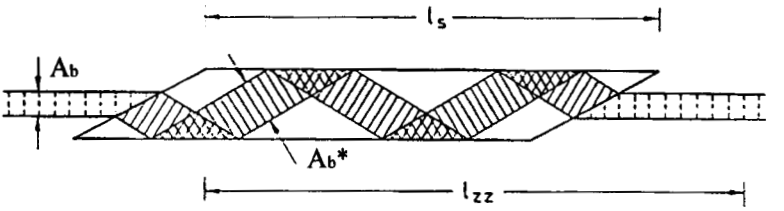

Fig. 10.11 Beam propagation in a solid state slab. The endfaces are cut at the Brewster angle [S.11].

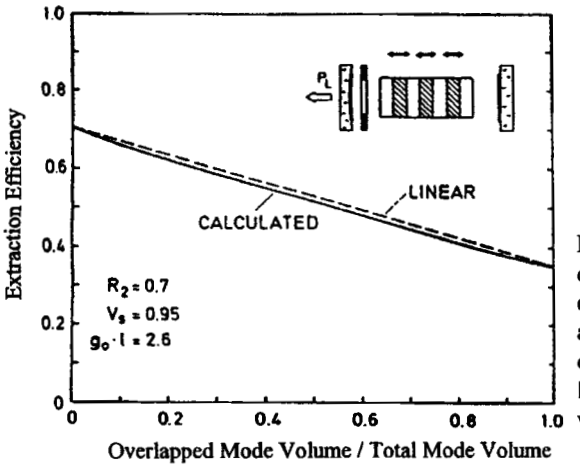

Fig. 10.12 Numerically calculated decrease of the extraction efficiency due to the beam overlap. The hatched areas mark the double pass areas. The decrease of the output power is almost linear with the overlapped mode volume [4.20] (© AIP 1988).

Incorporation of these three correction factors into Eq. (10.8) yields the general expression for the output power of folded resonators with a zig-zag path:

$$P_{out} = \gamma_1 \gamma_2 A_b I_S \frac{1-R}{1 - R + \sqrt{R}\,(1/V_S - V_S)} \left[\gamma_3 g_0 \ell - \left|\ln\sqrt{R V_S^2}\right|\right]$$

with: $V_S = \exp[-\alpha_0 \ell \gamma_3]$ (12.25)

a) Tightly Folded Resonator

Let us consider a slab with cross sectional area A, length ℓ, and index of refraction n. For complete beam overlap, which means that $(N+1)a=\ell\cos\alpha$ holds as shown in Fig. 10.10, the three correction factors as a function of the number of reflections N at the bottom surface read:

$$\gamma_1 = 1 - \frac{1}{2}\frac{2N-1}{2N+1} \tag{10.26}$$

$$\gamma_2 = \frac{A}{A_b}\sin\beta \tag{10.27}$$

$$\gamma_3 = \frac{2N}{N+1}\frac{1}{\sin\beta} \tag{10.28}$$

with: $\sin\alpha/\sin\beta = n$

The expression for the output power then reads:

$$P_{out} = \left[1-0.5\frac{2N-1}{2N+1}\right]\left[\frac{2N}{N+1}\right] A I_S \frac{1-R}{1-R+\sqrt{R}(1/V_S-V_S)} \left[g_0\ell-\alpha_0\ell-\frac{1}{\gamma_3}\left|\ln\sqrt{R}\right|\right] \tag{10.29}$$

For a high number of reflections N the product of the two first terms goes to 1.0. We then get the same slope efficiency as compared to a linear resonator whose beam penetrates the medium through the side face with cross section A, but the laser threshold is reduced by the factor $1/\gamma_3$. The lower laser threshold results in a higher extraction efficiency. This is shown in Fig. 10.13 in which extraction efficiencies for different reflection numbers N are compared. For high numbers N the maximum extraction efficiency is higher as compared to the linear resonator.

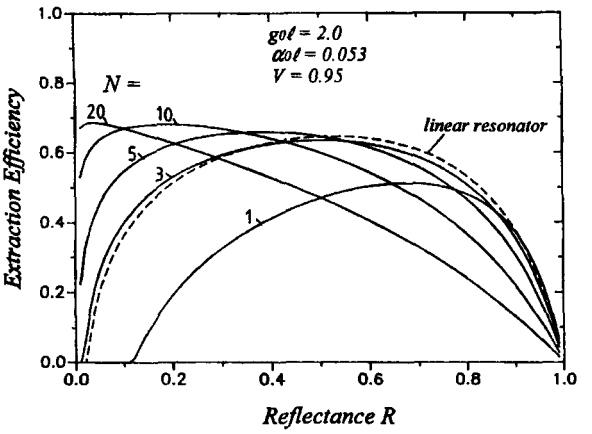

Fig. 10.13 Numerically calculated extraction efficiencies for tightly folded resonators with complete beam overlap as a function of the output coupling reflectance. A round trip diffraction loss factor V of 0.95 was used ($V_1=V_3=\sqrt{0.95}$, $V_2=V_4=1.0$, see Fig. 10.10). The differential equation (10.2) was solved.

b) Slab Resonator

The endfaces of the slab with index of refraction n and side length ℓ are cut at the Brewster angle $\alpha=atan(n)$ (Figs. 10.11 and 10.14). If a_0 denotes the width of the incoming beam and a is the width of the slab, the three correction factors read:

$$\gamma_1 = 1 - \frac{1}{2}\,\frac{1}{(8a/a_0)\cos^2\alpha - 1} \tag{10.30}$$

$$\gamma_2 = \tan\alpha \tag{10.31}$$

$$\gamma_3 = \frac{1}{\sin(2\alpha)} \tag{10.32}$$

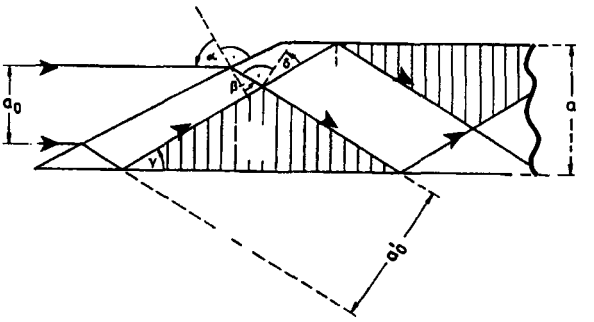

Fig. 10.14 Beam propagation inside a slab active medium. The hatched areas indicate the areas of beam overlap.

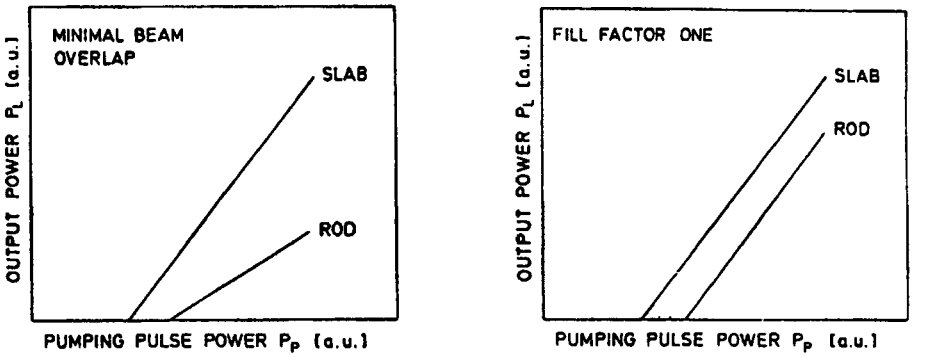

Fig. 10.15 Qualitative comparison of the output power of a Nd:YAG Brewster slab resonator and a linear Nd:YAG rod resonator for minimum and complete beam overlap in the slab (same side length, gain, loss, and cross sectional area of the active medium in both geometries) [4.20] (© AIP 1988).

Insertion into (10.25) yields:

$$P_{out} = \frac{1}{2\cos^2\alpha}\left[1 - \frac{1}{2}\frac{1}{(8a/a_0)\cos^2\alpha - 1}\right] A_b I_S \frac{1-R}{1-R+\sqrt{R}(1/V_S - V_S)}\left[g_0\ell - \alpha_0\ell - \sin(2\alpha)\left|\ln\sqrt{R}\right|\right]$$

with A_b: cross sectional area of the incident beam (10.33)

Again, we get a reduction of the laser threshold due to the longer optical path (factor $sin2\alpha$). If the width of the incident beam is much smaller than the slab width (fundamental mode operation), we get minimal beam overlap resulting in a factor γ_1 close to one. Compared to a linear resonator with active medium with length ℓ (same slab but without zig-zag), the slope is higher by $1/(2cos2\alpha)$ due to the increased mode volume inside the slab. For complete beam overlap, the slope is the same as for the linear resonator, but the laser threshold is still reduced by $sin2\alpha$. In any case, the slab configuration provides a higher output power as compared to a linear resonator (Fig. 10.15) [4.19-4.21].

10.1.4 Ring Resonators

Ring resonators are used to prevent spatial hole burning in the active medium. By using an optical isolator inside the resonator, the laser light is forced to travel in one direction only (Fig. 10.16). The missing counterpropagating beam prevents the formation of standing waves. With only one travelling wave, the amplification of the light in the active medium is described by a differential equation that is different from (10.2) for the linear resonator:

$$\frac{dI}{dz} = \left[\frac{g_0}{1 + I/I_S} - \alpha_0\right] I \tag{10.34}$$

Again, we can solve this equation analytically if we concentrate the losses $\alpha_0 \ell$ of the medium at one endface of the active medium. Starting at the output coupling mirror with intensity $I(0)$, the intensity $I(L)$ after one round trip must obey the stationary condition:

$$\frac{I(L)}{I(0)} = \frac{1}{V_1 V_2 V_3 V_4 R V_S} \tag{10.35}$$

with V_S=exp[$-\alpha_0 \ell$] and V_1-V_4 being diffraction loss factors per transit (=1-loss), as depicted in Fig. 10.16. By using this boundary condition, the solution of (10.34) yields the output power:

$$P_{out} = A_b\, I(L)\, (1-R) \tag{10.36}$$

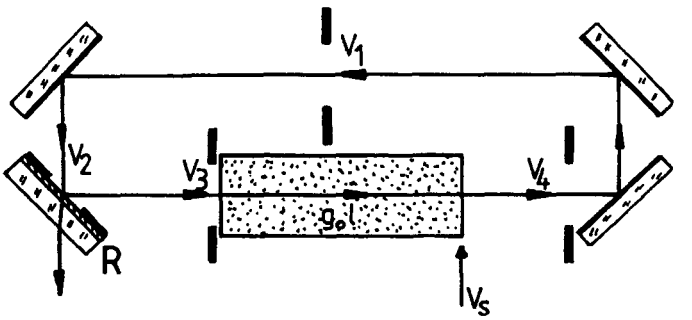

Fig. 10.16 Model of a ring resonator used for the calculation of the output power. The optical isolator generating the unidirectional beam propagation is not shown. Diffraction losses at the apertures are characterized by the loss factors V_1-V_4, and the loss of the medium is taken into account at the end of the medium by the loss factor V_S.

The final result reads:

$$P_{out} = A_b\, I_S\, \frac{(1-R)V_2}{1 - 1/(VV_SR)} \left[g_0\ell - |\ln(VV_SR)|\right] \tag{10.37}$$

with: $V = V_1V_2V_3V_4$

Compared to the corresponding expression for the linear resonator (10.7), we find an increased laser threshold due to the unidirectionality (the light is only amplified once per round trip). However, the maximum extraction efficiencies attainable are similar for both resonator schemes since the impact of the higher threshold on the output power can be compensated by increasing the mirror reflectance R. Figure 10.17 compares maximum extraction efficiencies $\eta_{extr,max}$ and optimum output coupling transmittances $T_{opt}=1-R_{opt}$ for linear resonators and ring resonators (see also Fig. 10.4). These graphs were generated by numerically solving the differential equation (10.2) and (10.34) with the corresponding boundary conditions. Compared to a linear resonator, optimized ring resonators require a lower output coupling to provide a similar output power for a given small-signal gain.

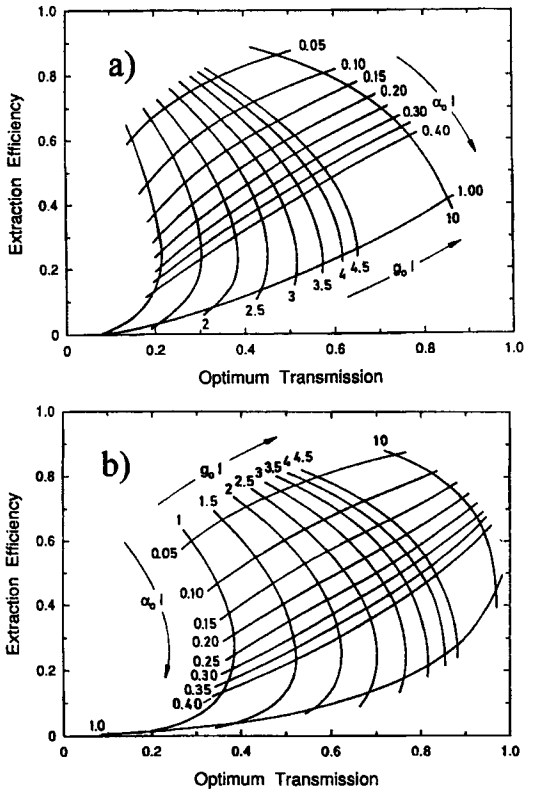

Fig. 10.17 Numerically calculated maximum extraction efficiencies and corresponding optimum mirror transmittances for homogeneously broadened lasers. The curve para-meters are the small-signal gain $g_0\ell$ and the loss per transit $\alpha_0\ell$. a) ring resonator, b) linear resonator.

10.2 Output Power of Unstable Resonators

In unstable resonators the differential equation (10.2) cannot be applied without modifications since the two counterpropagating beams do not overlap completely. Depending on the resonator geometry and the position of the active medium inside the resonator, an outer area exists in which the gain is only saturated by the back travelling wave (see hatched area in Fig. 10.18). Only in the central area of the medium (marked by I) is the inversion depleted in a similar way as in stable resonators, whereas the periphery of the active medium acts as an amplifier for the outcoupled field. Furthermore, the propagation of the diverging wave leads to a longitudinal intensity profile that is different from the one for stable resonators shown in Fig. 10.2. The intensity at the high reflecting mirror, for instance, is lower than the intensity at the output coupler although the light is being amplified by the active medium.

Fortunately, we can take the special beam propagation into account by modifying the differential equation (10.2) [4.9,4.14,4.16,4.18]. For a confocal unstable resonator as shown in Fig. 10.18 the equations read:

$$\frac{dI^+}{dz} = +\left[\frac{g_0}{1 + (I^+ + I^-)/I_S} - \alpha_0\right] I^+ - \frac{2I^+}{z+z_0} \tag{10.38}$$

$$\frac{dI^-}{dz} = -\left[\frac{g_0}{1 + (I^+ + I^-)/I_S} - \alpha_0\right] I^- \tag{10.39}$$

The numerical solution of these equations provides the intensities as a function of z. However, in the outer area marked by II, the intensity I also depends on the radial coordinate. This radial dependency has to be incorporated numerically by subdividing the medium into a sequence of disks with each disk having radial points at which the intensity is calculated.

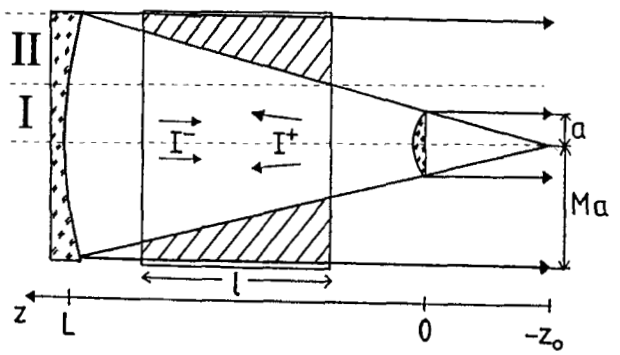

Fig. 10.18 Beam propagation in a confocal unstable resonator.

If the intensity $I^-(z,r)$ at $z=0$ is known as a function of the radius r, the output power P_{out}, extraction efficiency η_{extr}, and the loss factor V (due to output coupling) can be determined using the following relations (for a circular medium with radius Ma):

$$P_{out} = 2\pi \int_{a}^{Ma} I^-(0,r)\, r dr \tag{10.40}$$

$$\eta_{extr} = \frac{P_{out}}{\pi M^2 a^2 I_S g_0 \ell} \tag{10.41}$$

$$V = \frac{\pi a^2 I^-(0,0)}{\pi a^2 I^-(0,0) + P_{out}} \tag{10.42}$$

Since the amplification in the outer area is radially dependent, the output coupling loss is increased as the small-signal gain of the medium is increased. As shown in Fig. 10.19, the loss factor equals the geometrical loss factor $1/M^2$ only at the laser threshold and immediately decreases as the gain is increased. This is caused by the lower gain saturation in the periphery of the active medium which in turn leads to a higher intensity in the outer areas of the outcoupled beam profile. Remember that the loss factor V is caused by the output coupling and it therefore corresponds to the mirror reflectance in a stable resonator. The change in output coupling implies that the output power does not increase linearly with the input power, a well-known behavior of unstable laser resonators. The reader may argue that the geometrical model used is too rough since it neglects the true mode structure. However, in Chapter 11 we will incorporate diffraction into our output power model and obtain very similar results.

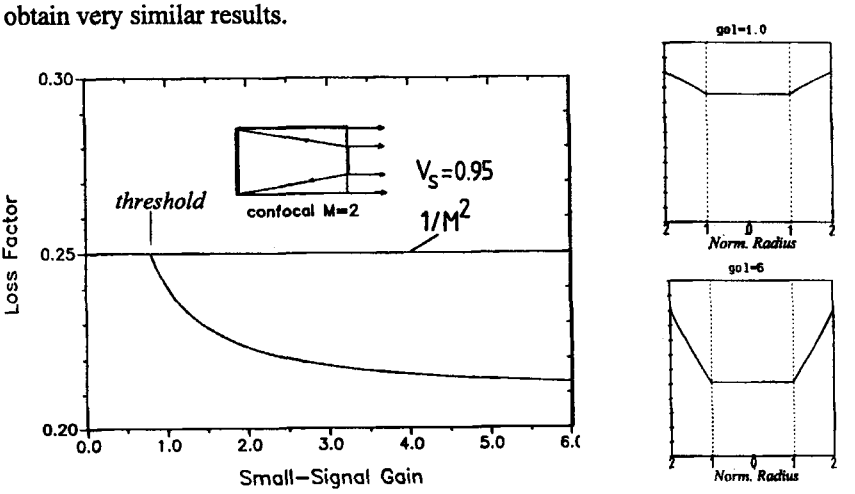

Fig. 10.19 Loss factor as a function of the small-signal gain calculated with Eq. (10.38)-(10.42) for a confocal unstable resonator with magnification $M=2$. The radial intensity profiles $I^-(0,r)$ at the plane of the output coupler are shown on the right side for two different small-signal gains.

The problem we are interested in is, of course, how the unstable resonator compares to the stable resonator as far as the maximum extraction efficiency is concerned. For a given unstable resonator with loss factor V we can calculate the output power of a stable resonator with mirror reflectance $R=V$ using the same active medium. A comparison of the output power will then reveal any influence of the special beam propagation in unstable resonators on the extraction efficiency. Some examples are shown in Fig. 10.20. We see that both resonator geometries provide similar extraction efficiencies as long as the area with one intensity (hatched area in Fig. 10.18) is kept small [4.16,4.18]. The preferred geometry would be to position the medium close to the high reflecting mirror. As soon as the medium is moved closer to the output coupler, the amplifier region becomes larger resulting in a decrease of the output power. However, as far as the maximum extraction efficiency is concerned, the location of the active medium does not really matter and both resonator schemes provide a similar performance. Thus we can apply (10.8) also to unstable resonators if we replace the mirror reflectance R with the loss factor V:

$$P_{out} = A_b\, I_S \frac{1-V}{1 - V + \sqrt{V}\,(1/V_S - V_S)} \left[g_0 \ell - \left|\ln\sqrt{V V_S^2}\right|\right] \qquad (10.43)$$

with $\quad A_b = \pi M^2 a^2$ (fill factor of one)

Keep in mind that the loss factor V is a function of the small-signal gain!

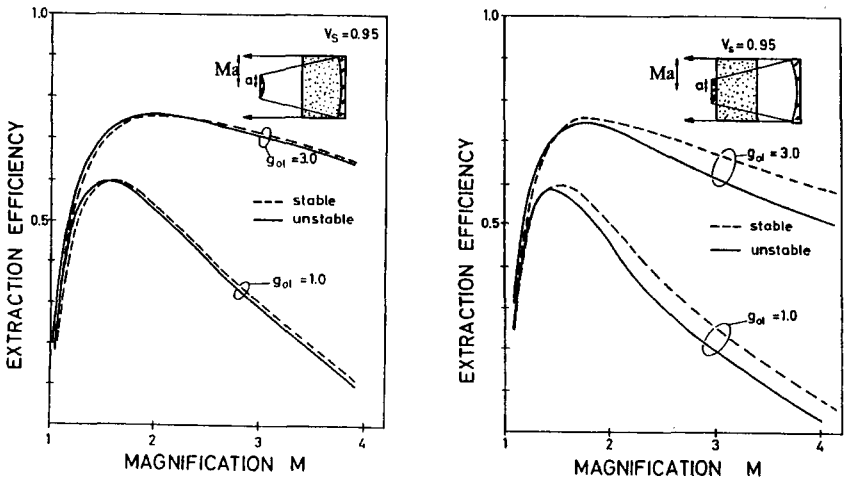

Fig. 10.20 Calculated extraction efficiency of confocal unstable resonators as a function of the magnification for different small-signal gains and different locations of the active medium. The broken line represents the extraction efficiency of a stable resonator exhibiting the same output coupling.